Journal of Statistical Physics, Vol. 86, Nos. 3/4, 1997

Effective Medium Approximation for Strongly Nonlinear Media

Leora Sali[1,2] **and David J. Bergman**[1]

Received January 22, 1996; final July 8, 1996

The effective medium approximation is one of the most popular approximations used for calculating the effective coefficients of linear composite media. When the same approach is applied to the case of power-law nonlinear composite media the obtained expression contains a function whose values are unknown. In order to determine the form of this function and to calculate some coefficients related to it, we calculate the electric field for the case of a single inclusion. The numerical solution is based on the relaxation method for solving differential equations, but involves some modifications due to the nonlinearity. After the solution of the differential equation the function and the coefficients are calculated and examined. The results differ considerably from those obtained earlier by simple approximations.

KEY WORDS: The effective medium theory; nonlinear behavior; composite medium; strong nonlinearity; bulk effective moduli; bulk effective conductivity.

1. INTRODUCTION

Nonlinear composite materials have attracted much interest in the last few years. The problem of calculating the bulk effective properties of these materials is in general quite intractable, since it involves the solution of a nonlinear partial differential equation with coefficients that depend on position in a way that reflects the detailed microgeometry. Thus, a variety of approximations have been devised to solve the problem in certain limits. In order to discuss a composite medium made of *weakly nonlinear* components, Stroud and Hui[1] used a perturbation expansion in order to

[1] School of Physics and Astronomy, Raymond and Beverly Sackler Faculty of Exact Sciences, Tel Aviv University, Tel Aviv 69978, Israel; e-mail: bergman@star.tau.ac.il.
[2] Present address: 11 Kaplan St., Yehud, Israel 56251.

0022-4715/97/0200-0455$12.50/0

obtain results, exact to first order in the nonlinear (cubic) susceptibility of the components, for dilute concentrations of inhomogeneities. That discussion has been extended to nondilute concentrations of inhomogeneities, using mean-field theory.[2,3] Scaling theories were developed for describing the critical behavior of such systems near a percolation threshold.[4,5]

For composite media made of components that are *strongly nonlinear* Blumenfeld and Bergman[6] obtained a result for the effective dielectric constant which is exact to second order in the fluctuations (contrast) of the dielectric coefficients of the components. Another approximation that was used is based on a variational method[7–9] which is not limited to special perturbation limits or to special types of nonlinearities.

One of the most widely used approximations for calculating the bulk effective electrical conductivity of a two-component composite medium is the effective medium approximation (EMA), which was invented by Bruggeman in 1935.[10] Bruggeman's approximation applies without any change also to the dielectric permittivity, magnetic permeability, thermal conductivity, and chemical diffusivity coefficients, since the mathematical structure of the associated physical properties is the same as that of electrical conduction.

Bruggeman's approximation was reformulated in a different way,[11] showing that the result does not depend on the kind of averaging used. The procedure was then generalized to the case of nonlinear properties of composites and applied to a case of a strongly nonlinear composite conductor. In that case each component exhibits an isotropic power-law relation between the electric field $\mathbf{E}(\mathbf{r})$ and the current density $\mathbf{J}(\mathbf{r})$, where the nonlinearity exponent β [see (2.1) below] has the same value in all components. The equation that was found to embody the EMA for the nonlinear effective conductivity σ_e contains an unknown function $f(x)$, where x is the ratio between the nonlinear conductivity coefficients of the two components. The form of-the critical behavior of σ_e near the percolation threshold was determined, and it was found to have scaling properties. The results included four constants, which are related to the behavior of $f(x)$ for x near 0 and x near ∞. The exponents which characterize the critical behavior were found to depend upon β, although the values obtained for them in this approximation are not expected to be accurate, just as in the linear case $\beta = 0$ (see, e.g., ref. 12).

In order to get an explicit form for the nonlinear EMA, we need to calculate the function $f(x)$ for different values of x. Moreover, in order to complete the calculation of the scaling properties, the four constants mentioned above also need to be determined. To achieve these goals, we need a detailed, explicit solution for the nonuniform field $\mathbf{E}(\mathbf{r})$ which is present when a single spherical inclusion is placed in an otherwise uniform host

medium and an external field is applied that is uniform far away from the inclusion.

In this article we review the nonlinear EMA for continuous media which was derived in ref. 11. We then formulate an equivalent nonlinear EMA for conductance networks. The problem of a single inclusion is first tackled in the context of the nonlinear network model, where it is significantly easier than in the continuum case. After that we also solve the continuum problem of a single spherical inclusion in an infinite host medium, using a relaxation algorithm which was developed especially for this task. These solutions provide us with an evaluation of $f(x)$ and of the four constants for different values of the nonlinearity exponent for both the network model and the continuum system. Using these as building blocks, we can now apply EMA to any composite medium with a power-law nonlinear constitutive relation of the form (2.1).

2. NONLINEAR EMA

2.1. Review of Nonlinear EMA for Continuous Media

In this section we summarize some relevant results which were derived in detail in ref. 11.

We consider a composite conducting medium where each component exhibits an isotropic power-law relation between the electric field $\mathbf{E}(\mathbf{r})$ and the current density $\mathbf{J}(\mathbf{r})$ of the form

$$\mathbf{J} = \sigma |\mathbf{E}|^{\beta} \mathbf{E} \tag{2.1}$$

The nonlinearity exponent $\beta > -1$ has the same value in all components, and the difference between them is only in the value of the nonlinear conductivity coefficient σ. The expression for the bulk effective nonlinear conductivity coefficient in this case is

$$\sigma_e = \frac{1}{V} \int dV \, \sigma(\mathbf{r}) \left| \frac{\mathbf{E}(\mathbf{r})}{\mathbf{E}_0} \right|^{\beta+2} \tag{2.2}$$

The determination of $\mathbf{E}(\mathbf{r})$ requires numerical solution of a nonlinear partial differential equation for the scalar potential $\phi(\mathbf{r})$:

$$\nabla \cdot (\sigma(\mathbf{r}) |\nabla \phi|^{\beta} \nabla \phi) = 0 \tag{2.3}$$

In order to obtain an EMA for σ_e, we consider a large volume V of a homogeneous conductor σ_0 with a single spherical inclusion σ_i of volume

$V_a \ll V$. Equation (2.3) cannot be solved analytically for this case, even when restricted to $\mathcal{O}(V_a/V)$ terms. However, from the homogeneity properties of $\sigma_e(\sigma_0, \sigma_i)$ we can conclude that σ_e has the form

$$\sigma_e = \sigma_0 + \sigma_0 \frac{V_a}{V} f\left(\frac{\sigma_0}{\sigma_i}\right) + \mathcal{O}\left(\frac{V_a^2}{V^2}\right) \tag{2.4}$$

where $f(x)$ is a function which remains to be determined. Imposing the consistency requirement that the average of σ_e over the various types of inclusions be equal to σ_0 leads to an equation that defines the EMA for the nonlinear effective conductivity σ_e. The fluctuations which are averaged in this procedure are of order V_a/V and thus very small compared to σ_0; therefore it is immaterial what kind of averaging is used. In the case of a two-component composite the EMA equation is

$$p_1 f\left(\frac{\sigma_e}{\sigma_1}\right) + (1 - p_1) f\left(\frac{\sigma_e}{\sigma_2}\right) = 0 \tag{2.5}$$

The percolation threshold p_c in this approximation can be easily found by considering the case of large contrast between the components. Near the threshold we expect to find $\sigma_2 \ll \sigma_e \ll \sigma_1$. Using these inequalities in (2.5), we obtain

$$p_c = \frac{f(\infty)}{f(\infty) - f(0)} \tag{2.6}$$

In order to determine the behavior of σ_e near p_c, the forms of $f(x)$ were determined for x near 0 and x near ∞. For small $x = \sigma_0/\sigma_1$ it was shown that

$$f(x) \simeq f(0) - a(\beta + 1)\, x^{1/(\beta+1)} \tag{2.7}$$

$$f(0) = \frac{1}{V_a} \int dV\, \theta_0 \left(\left| \frac{\mathbf{E}(\mathbf{r})}{E_0} \right|^{\beta+2} - 1 \right) - 1 \tag{2.8}$$

$$a = \lim_{\sigma_0/\sigma_1 \to 0} \frac{1}{V_a} \int dV\, \theta_1 \left| \frac{\mathbf{E}(\mathbf{r})}{E_0} \right|^{\beta+2} \left(\frac{\sigma_1}{\sigma_0} \right)^{(\beta+2)/(\beta+1)} \tag{2.9}$$

Here the functions $\theta_0(\mathbf{r})$ and $\theta_1(\mathbf{r})$ are the characteristic functions of the host medium and of the inclusion, respectively. Both $f(0)$ and a are $\mathcal{O}(1)$, and $f(0) > 0$ since $\sigma_1 > \sigma_0$ for x near 0.

For large $x=\sigma_0/\sigma_2$ it was found that [note that, even though (2.8) and (2.11) appear to be identical, the local field $\mathbf{E}(\mathbf{r})$ is different, therefore also $f(\infty)\neq f(0)$]

$$f(x)\simeq f(\infty)+\frac{b}{x} \tag{2.10}$$

$$f(\infty)=\frac{1}{V_a}\int dV\,\theta_0\left(\left|\frac{\mathbf{E}(\mathbf{r})}{E_0}\right|^{\beta+2}-1\right)-1 \tag{2.11}$$

$$b=\frac{1}{V_a}\int dV\,\theta_2\left|\frac{\mathbf{E}(\mathbf{r})}{E_0}\right|^{\beta+2} \tag{2.12}$$

As before, $\theta_0(\mathbf{r})$ and $\theta_2(\mathbf{r})$ are the characteristic functions of the host medium and of the inclusion, respectively. Both $f(\infty)$ and b are $\mathcal{O}(1)$, and $f(\infty)<0$ since $\sigma_2<\sigma_0$ for x near ∞.

In Section 4 we will describe a numerical calculation of the electric field for the above-mentioned configuration: a small spherical inclusion embedded in a large homogeneous host medium. Using the solutions for $\mathbf{E}(\mathbf{r})$ at different values of x, we then compute the function $f(x)$ and evaluate the four coefficients $f(0)$, $f(\infty)$, a, and b for different values of β.

2.2. Nonlinear EMA for Conductance Networks

In this section we formulate an EMA for conductance networks in a way that is very similar to the one used for continuous media. Consider a three-dimensional simple cubic resistor networks that has a total of N_x resistors oriented in parallel to the x axis, and similarly N_y and N_z resistors oriented along the y and z axes, respectively. A pair of equipotential plates perpendicular to the x axis and with potential difference ΔV determine the boundary conditions for the network. For a single nonlinear resistor we have

$$I=V\cdot|V|^{\beta}\cdot g \tag{2.13}$$

where I is the current through tithe resistor, V is the voltage across it, and g is the nonlinear conductance coefficient.

The bulk effective conductance g_e of an inhomogeneous nonlinear network is defined as the nonlinear conductance of a single resistor such that if we replace all the resistors in the network with it, it will produce the same dissipation rate as in the actual inhomogeneous network. The dissipation rate of a nonlinear resistor is

$$P=|V|^{\beta+2}\cdot g \tag{2.14}$$

Therefore we can compare the total dissipation rate of an inhomogeneous network to that of a homogeneous network with g_e for all resistors and obtain for the nonlinear effective conductance

$$g_e = \frac{1}{N_x} \sum_{xyz} g_i \left| \frac{V_i}{V_0} \right|^{\beta+2} \tag{2.15}$$

where the sum is over *all* the resistors, $V_0 = \Delta V / N_x$, and V_i and g_i are, respectively, the voltage across and the conductance of the resistor i.

In order to obtain an EMA for g_e, we will consider a conductance network in which all the resistors have the same nonlinear conductance g_0 except for one resistor (henceforth to be called the inclusion), with conductance g_i, which lies along the x axis. Here, too, we cannot calculate g_e in closed form, but from the homogeneity properties of $g_e(g_0, g_i)$ we conclude that g_e has the form

$$g_e = g_0 + g_0 \frac{1}{N_x} f\left(\frac{g_0}{g_i}\right) + \mathcal{O}\left(\frac{1}{N_x^2}\right) \tag{2.16}$$

where $f(x)$ is a function which remains to be determined. Imposing the consistency requirement that the average of g_e over the various types of inclusions be equal to g_0, we get the following EMA equation for a network composed of two types of resistors in which the fraction of g_1 resistors is p_1:

$$p_1 f\left(\frac{g_e}{g_1}\right) + (1 - p_1) f\left(\frac{g_e}{g_2}\right) = 0 \tag{2.17}$$

As in the case of a continuous medium; we find for the percolation threshold

$$p_c = \frac{f(\infty)}{f(\infty) - f(0)} \tag{2.18}$$

As before, in order to determine the behavior of g_e near p_c, we need to know the forms of $f(x)$ for x near 0 and x near ∞. For small x we observe that when $g_0 \ll g_1$, a qualitative consideration leads to the result that the magnitude of V_i, the voltage across a resistor, satisfies

$$\left| \frac{V_i}{V_0} \right|^{\beta+1} \propto \begin{cases} g_0/g_1 & \text{for the inclusion } g_1 \\ 1 & \text{for a resistor } g_0 \end{cases} \tag{2.19}$$

Expressing g_i with the help of the characteristic function of the majority resistors, θ_0, and that of the inclusion, θ_1,

$$g_i = g_0\theta_0 + g_1\theta_1 \tag{2.20}$$

we can rewrite (2.15) as

$$\frac{g_e}{g_0} = \frac{1}{N_x}\sum_{xyz}\left(\theta_0 + \frac{g_1}{g_0}\theta_1\right)\left|\frac{V_i}{V_0}\right|^{\beta+2} \tag{2.21}$$

which is a function only of g_1/g_0. Using (2.19) to estimate the two terms in (2.21) and comparing the result with (2.16), we get, for $x \ll 1$,

$$f(x) \simeq f(0) - a(\beta+1)\,x^{1/(\beta+1)} \tag{2.22}$$

$$f(0) = \sum_x \theta_0\left(\left|\frac{V_i}{V_0}\right|^{\beta+2} - 1\right) + \sum_{yz}\theta_0\left|\frac{V_i}{V_0}\right|^{\beta+2} - 1 \tag{2.23}$$

$$a = \lim_{g_0/g_1 \to 0}\sum_x \theta_1\left|\frac{V_i}{V_0}\right|^{\beta+2}\left(\frac{g_1}{g_0}\right)^{(\beta+2)/(\beta+1)} \tag{2.24}$$

where the sums $\sum_x$, $\sum_{yz}$ include all resistors lying along the designated axes. Both $f(0)$ and a are $\mathcal{O}(1)$, and $f(0) > 0$ since $g_1 > g_0$ entails $g_e > g_0$.

For large x we note that when $g_0 \gg g_2$, the inclusion is actually an insulator, which leads to the following result for the magnitude of V_i:

$$\left|\frac{V_i}{V_0}\right|^{\beta+1} \propto 1 \qquad \text{for all resistors} \tag{2.25}$$

Proceeding by analogy with (2.20)–(2.24), we write

$$g_i = g_0\theta_0 + g_2\theta_2 \tag{2.26}$$

$$\frac{g_e}{g_0} = \frac{1}{N_x}\sum_{xyz}\left(\theta_0 + \frac{g_2}{g_0}\theta_2\right)\left|\frac{V_i}{V_0}\right|^{\beta+2} \tag{2.27}$$

and finally eve get, for $x \gg 1$,

$$f(x) \simeq f(\infty) + \frac{b}{x} \tag{2.28}$$

$$f(\infty) = \sum_x \theta_0\left(\left|\frac{V_i}{V_0}\right|^{\beta+2} - 1\right) + \sum_{yz}\theta_0\left|\frac{V_i}{V_0}\right|^{\beta+2} - 1 \tag{2.29}$$

$$b = \sum_x \theta_2\left|\frac{V_i}{V_0}\right|^{\beta+2} \tag{2.30}$$

As before, both $f(\infty)$ and b are $\mathcal{O}(1)$, while $f(\infty) < 0$ since $g_2 < g_0$ entails $g_e < g_0$.

3. RESULTS FOR CONDUCTANCE NETWORKS

3.1. Kirchhoff's Equations

In this subsection we describe the method used for solving the equations of the conductance networks and for the calculation of g_e and the EMA coefficients.

In order to calculate g_e according to (2.15), we need to know the voltages across all the resistors in the network. In a three-dimensional simple cubic network there are six resistors around each internal node. If we take V_i to be the voltage across a resistor, g_i to be its nonlinear conductance, and I_i to be the current through it, then the current conservation condition at an internal node becomes

$$\sum_{i=1}^{6} I_i = \sum_{i=1}^{6} V_i^{\beta+1} \cdot g_i = 0 \tag{3.1}$$

These are just Kirchhoff's current equations for the nonlinear system. If we wish to generalize (3.1) for nodes on the sidewalls of the network, we can define fictitious zero currents for the side where there is no resistor. The boundary conditions for the system are derived from the uniform potential plates: The potentials at all nodes of one boundary differ by ΔV from the ones at the opposite boundary. If we solve (31) for all the nodes with the given boundary conditions, we will have the voltages across all resistors. Using those voltages in (2.15), we will then calculate the effective conductance.

3.2. The Relaxation Method

Kirchhoff's equations express the fact that the potential at a certain node depends on the potentials at the six surrounding nodes. The common numerical method for this kind of problem is the relaxation method.[13] Using this method, we calculate an updated potential for each node, using the previous values for the neighboring nodes. This procedure is iterated until convergence is achieved. The detailed procedure is as follows: Taking ϕ to be the previous potential of a node, ϕ_i to be the previous potentials at the surrounding nodes ($i = 1,..., 6$), and $\tilde{\phi}$ to be the corresponding solution

of Kirchhoff's equations for the potential at the central node, we calculate an updated potential at the central node $\tilde{\phi}_0$ by

$$\tilde{\phi}_0 = \phi + (\tilde{\phi} - \phi)\, w \tag{3.2}$$

where w is a relaxation coefficient whose value lies between 0 and 2. This method is commonly used for linear problems. In that case, the relation between $\tilde{\phi}$ and ϕ_i is a linear function. In our case that function is nonlinear and quite complicated; therefore $\tilde{\phi}$ is evaluated numerically using the Newton–Raphson method. In order to use this method, we need to be able to calculate this function and its derivative everywhere. The Newton–Raphson method is usually applied iteratively; however, in our case, even if we found an exact local solution for $\tilde{\phi}$ and $\tilde{\phi}_0$ at each node, this solution would still be only an approximate global solution. Therefore, at each node only one step of the Newton–Raphson iteration is executed.

The nonlinear function whose zero we want to find is

$$F(V) \equiv \sum_{i=1}^{6} (V_i - V)\, |V_i - V|^{\beta}\, g_i \tag{3.3}$$

Using the function and its derivative, we obtain a new value for ϕ at any node by

$$\tilde{\phi}_0 = \phi - w \frac{F(\phi)}{F'(\phi)} = \phi + w \frac{\sum_{i=1}^{6} (\phi_i - \phi)\, |\phi_i - \phi|^{\beta}\, g_i}{\sum_{i=1}^{6} (\beta + 1)\, |\phi_i - \phi|^{\beta}\, g_i} \tag{3.4}$$

After the new value $\tilde{\phi}_0$ is determined it is saved in an array of potentials. During the relaxation this process is executed for all the nodes of the network in each iteration. When it has converged we get the values of ϕ that solve Kirchhoff's equations. We then use this solution to calculate the effective conductance of the network using (2.15), and also to calculate the other coefficients of the EMA.

The parameters that were held fixed during all the calculations are the conductance of the host conductors and the network size, which was 20 resistors in each direction. The parameters that were allowed to change are the nonlinearity coefficient β and the conductance of the inclusion resistor.

3.3. Testing the Algorithm

A set of numerical calculations was made, using double precision (eight byte) real variables, in order to test the numerical algorithm. In the linear case $\beta = 0$ the effective conductance can be calculated in closed form

for a large hypercubic network where all the resistors are g_0 except for one inclusion g_1.[14] For a d-dimensional network we find that

$$\frac{V_1}{V_0} = \frac{d}{g_1/g_0 + d - 1} \tag{3.5}$$

where V_1 is the voltage across the inclusion. We can use this result together with Eq. (2.15) in order to obtain an explicit expression for the effective conductance g_e,

$$\frac{g_e}{g_0} = 1 + \frac{d}{N_x} \frac{g_1 - g_0}{g_1 + g_0(d-1)} \tag{3.6}$$

We can also use (3.5) and (3.6) in order to obtain explicit values for a, b, $f(0)$, and $f(\infty)$:

$$a = d^2 \tag{3.7}$$

$$b = \left(\frac{d}{d-1}\right)^2 \tag{3.8}$$

$$f(0) = d \tag{3.9}$$

$$f(\infty) = -\frac{d}{d-1} \tag{3.10}$$

The results for g_e from numerical computations at $d = 3$ were compared with these exact expressions. The differences were found to be of order 10^{-8}. This can be compared to $g_e/g_0 - 1$, which was about 10^{-4}, reflecting the fact that $N_x = 20^3 = 8000$.

3.4. Calculation of the EMA Coefficients for Conductance Networks

The aim of the main set of calculations was to compute the coefficients for different values of the nonlinearity exponent β. In all the calculations all the resistors were equal except for one inclusion. The conductance of the host resistors was $g_0 = 1$ and that of the inclusion resistor varied from 10^{-8} to 10^6 by factor-10 steps. The calculations were executed for values of $\beta = 0, 1, 2, 3$, using a relaxation coefficient $w = 1.7$, which corresponds to overrelaxation.

Figure 1 shows the calculated coefficients a, b, $f(0)$, and $f(\infty)$ for different values of β. The values obtained numerically for $\beta = 0$ are very close to the exact results (3.7)–(3.10).

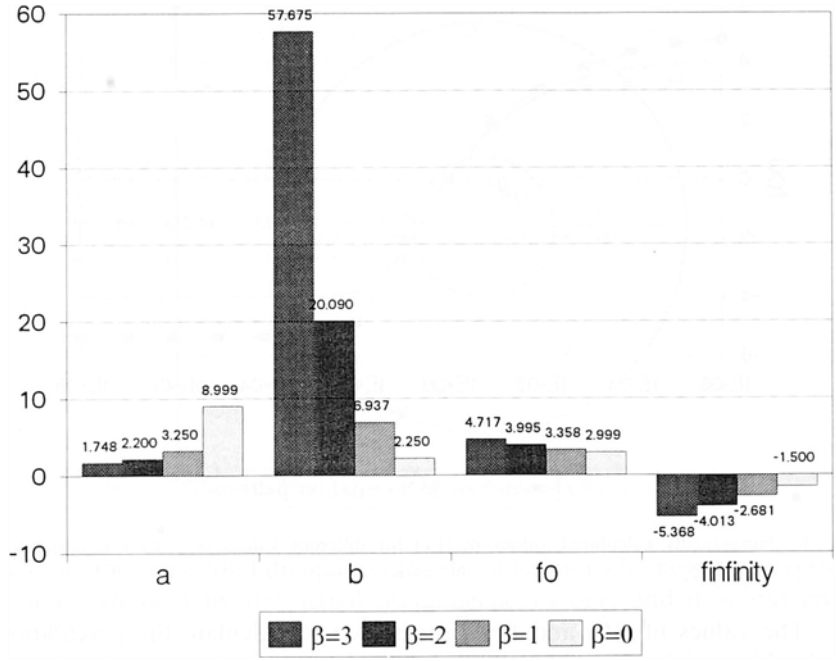

Fig. 1. Values of a, b, $f(0)$, and $f(\infty)$ plotted for different values of β.

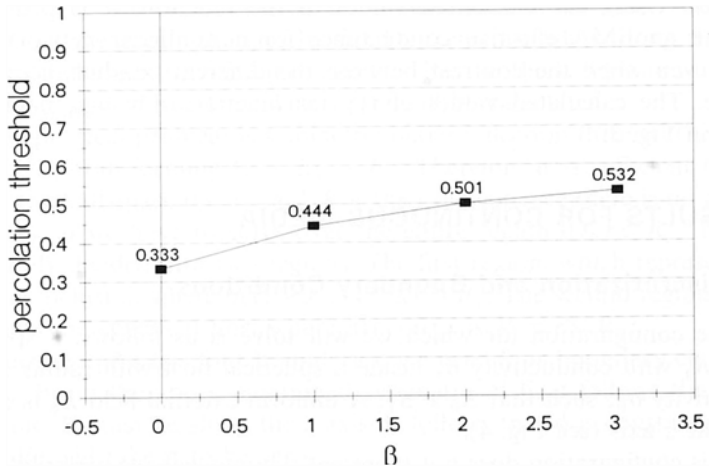

Fig. 2. The calculated percolation threshold plotted as function of β for a conductance network.

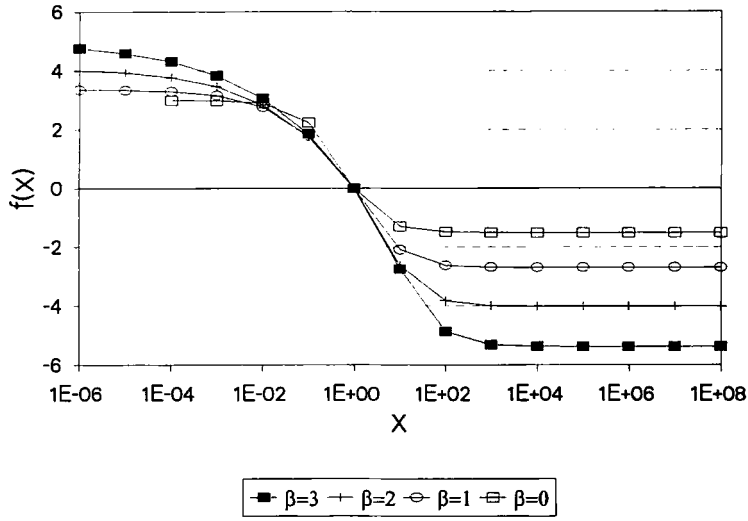

Fig. 3. Numerically calculated values of $f(x)$ for different values of β in a conductance network.

The values of $f(0)$ and $f(\infty)$ were used to calculate the percolation threshold according to (2.18), and the results are displayed in Fig. 2 as a function of β.

Since the effective conductance was calculated for all cases, the function $f(x)$ could be found for all values of x that were used, with the help of (2.16). Using the calculated values of the function, it is possible to calculate an EMA effective conductance for a nonlinear network using (2.17), even when the contrast between the different conductances is not extreme. The calculated values of $f(x)$ as function of $x = g_0/g_1$ are displayed in Fig. 3.

4. RESULTS FOR CONTINUOUS MEDIA

4.1. Discretization and Boundary Conditions

The configuration for which we will solve is as follows: a sphere of radius R_1 with conductivity σ_1 inside a spherical host with radius R_0 and conductivity σ_0, such that $R_0 \gg R_1$. A uniform external field E_0 is applied along the z axis (see Fig. 4).

This configuration does not represent a homogeneous material on any scale, and therefore the intuitive concept of a bulk effective conductivity is somewhat problematic. Nevertheless, σ_e is still defined by the property of

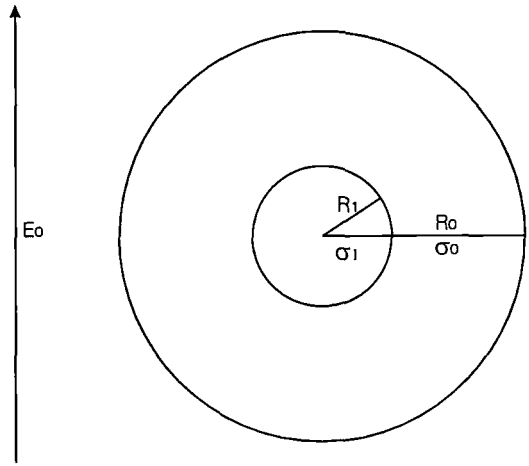

Fig. 4. Schematic illustration of the configuration for which we solve.

yielding the same total dissipation rate for a fictitious homogeneous system that is exhibited by the actual inhomogeneous one, and it is still given by (2.2).

The problem exhibits azimuthal symmetry. Therefore, if we use spherical coordinates, it is transformed into a two-dimensional problem, since the electric potential $\phi(r, \theta)$ is independent of the azimuthal angle φ. In order to solve the problem numerically, we must first discretize it. The electric potential $\phi(\mathbf{r})$ will be calculated on a two-dimensional grid. Along one direction of the grid r changes by fixed increments, while along the other direction θ changes by fixed increments. Thus, in the r, θ plane we have a rectangular grid of points at which $\phi(\mathbf{r})$ will be calculated.

The physical problem is symmetric under reflection through the origin, with E_x, E_y transforming to $-E_x, -E_y$. Therefore it is sufficient to solve just for the half-space $0 \leqslant \theta \leqslant \pi/2$. For the r dependence there is no obvious symmetry so we have to solve over the entire region $0 \leqslant r \leqslant R_0$. The grid is naturally divided into two regions. The first region, which represents the spherical inclusion where $\sigma(\mathbf{r}) = \sigma_1$, is $0 \leqslant r \leqslant R_1$. The second region, which represents the spherical host where $\sigma(\mathbf{r}) = \sigma_0$, is $R_1 \leqslant r \leqslant R_0$.

Since the grid has four boundaries, we need four boundary conditions for $\phi(\mathbf{r})$. From the above-mentioned symmetry of $\mathbf{E}$, it follows that in the x, y plane, $\mathbf{E}$ must lie along the z axis. It follows that ϕ is constant on that plane. We will take it to be zero,

$$\phi(r, \theta = \pi/2) = 0 \tag{4.1}$$

Another boundary of the grid, which is also in the x, y plane, corresponds to the single point $r = 0$; therefore we get the second boundary condition

$$\phi(r = 0, \theta) = 0 \tag{4.2}$$

At $r = R_0$ we assume that the field distortion due to the inclusion is negligible; therefore the potential there is only due to the external field

$$\phi(r = R_0, \theta) = -E_0 R_0 \cos\theta \tag{4.3}$$

The only boundary for which the value of the potential is unknown is the z axis, where $\theta = 0$. However, we know that the field there must be parallel to the z axis; thus the θ component of $\mathbf{E}$ vanishes,

$$\left.\frac{\partial\phi(r, \theta)}{\partial\theta}\right|_{\theta=0} = 0 \tag{4.4}$$

We do not have to explicitly impose any continuity conditions at the interface: Those are automatically enforced when the partial differential equation is satisfied at the interface.

4.2. Relaxation Method

In order to calculate the effective conductivity, we have to solve (2.3) with the given boundary conditions. The method chosen for this purpose is based on the relaxation method.[13] In this case we have to calculate a new potential for each point in the grid, using the old values of the potential in the neighboring points, such that $\nabla \cdot \mathbf{J} = 0$. This procedure is iterated until convergence is achieved. The expression $\nabla \cdot \mathbf{J}$ is related to the electric potential by

$$\nabla \cdot \mathbf{J} = \nabla \cdot (\sigma(\mathbf{r})\, |\nabla\phi|^{\beta}\, \nabla\phi) \tag{4.5}$$

If we try to express $\nabla \cdot \mathbf{J}$ at a point of the grid using the potential there and in the neighboring points, we get a complicated nonlinear expression. The value of the potential at that point cannot be found in closed form. Therefore, in contrast with the relaxation method for linear equations, here we must again use the Newton–Raphson method to find the new value of the potential at a grid point. Again, we need to be able to calculate a function and its derivative everywhere. We are interested, of course in finding the zero of

$$F(\phi_{i,j}) \equiv \nabla \cdot \mathbf{J} \tag{4.6}$$

where $\phi_{i,j}$ is the potential at the grid point (i, j) and $F(\phi_{i,j})$ also depends on the potentials at neighboring points. In order to calculate $F(\phi_{i,j})$, we use (4.5), and since r and θ change in the i and j directions, respectively, we get

$$\begin{aligned} F(\phi_{i,j}) &= \frac{(i+1/2)^2 \sigma_{i+1/2,j} |\mathbf{E}|^{\beta}_{i+1/2,j} E_{r_{i+1/2,j}} - (i-1/2)^2 \sigma_{i-1/2,j} |\mathbf{E}|^{\beta}_{i-1/2,j} E_{r_{i-1/2,j}}}{i^2 \Delta r} \\ &+ \frac{\sin[(j+1/2)\Delta\theta]\, \sigma_{i,j+1/2} |\mathbf{E}|^{\beta}_{i,j+1/2} E_{\theta_{i,j+1/2}}}{i \Delta r \Delta\theta \sin(j\Delta\theta)} \\ &- \frac{\sin[(j-1/2)\Delta\theta]\, \sigma_{i,j-1/2} |\mathbf{E}|^{\beta}_{i,j-1/2} E_{\theta_{i,j-1/2}}}{i \Delta r \Delta\theta \sin(j\Delta\theta)} \end{aligned} \tag{4.7}$$

In order to calculate this expression at a point (i, j) we need to use values of E_r at two points, $(i+1/2, j)$, $(i-1/2, j)$, and values of E_θ at two other points $(i, j+1/2)$, $(i, j-1/2)$. In reality, these points are not found on the grid, which includes only integer-valued pairs (i, j). However, since the potential is known at all of these latter points, we define

$$\begin{aligned} E_{r_{i+1/2,j}} &\equiv \frac{\phi_{i,j} - \phi_{i+1,j}}{r_{i+1} - r_i} \\ E_{\theta_{i,j+1/2}} &\equiv \frac{\phi_{i,j} - \phi_{i,j+1}}{r_i(\theta_{j+1} - \theta_j)} \end{aligned} \tag{4.8}$$

We also need to use $|\boldsymbol{E}|^2 = \mathrm{E}_r^2 + \mathrm{E}_\theta^2$ at the same four fictitious or half-integer points. In order to do this, we calculate quantities like $E_{r_{i,j+1/2}}$, $E_{\theta_{i+1/2,j}}$ by averaging over four neighboring values like (4.8),

$$|\mathbf{E}|^2_{i+1/2,j} = E^2_{r_{i+1/2,j}} + \left(\frac{E_{\theta_{i,j-1/2}} + E_{\theta_{i,j+1/2}} + E_{\theta_{i+1,j-1/2}} + E_{\theta_{i+1,j+1/2}}}{4}\right)^2 \tag{4.9}$$

$$|\mathbf{E}|^2_{i,j+1/2} = \left(\frac{E_{r_{i-1/2,j}} + E_{r_{i+1/2,j}} + E_{r_{i-1/2,j+1}} + E_{r_{i+1/2,j+1}}}{4}\right)^2 + E^2_{\theta_{i,j+1/2}} \tag{4.10}$$

This averaging procedure is correct for the interior regions of the host and the inclusion, but is problematic at the interface, due to the discontinuity of E_r. If we take $i = i_b$ to be the maximal i index such that the point (i, j) is still inside the inclusion, then at points such as $(i_b \pm 1/2, j)$ we can use (4.9), since the averaging is over E_θ, which is continuous at the boundary. On the other hand, at points like $(i_b, j+1/2)$ we cannot use (4.10),

since the averaging is over E_r, which has a jump discontinuity. Therefore, at those points we use a different scheme of averaging, with values of E_r taken only from points inside the inclusion

$$|\mathbf{E}|^2_{i_h, j+1/2} \equiv \left(\frac{E_{r_{i_h}-1/2, j} + E_{r_{i_h}-1/2, j+1}}{2} \right)^2 + E^2_{\theta_{i_h}, j+1/2} \tag{4.11}$$

Note that a similar special definition is *not needed* for $|\mathbf{E}|^2_{i_h+1, j+1/2}$ because in that case (4.10) only uses values of E_r at points that are outside the spherical inclusion.

Since $F(\phi_{i,j})$ is nonlinear and quite complicated, we use a numerical method to calculate its derivative: we first calculate the value of F for the current potential, then we add a small value δ to the potential and recalculate F. In this way we obtain the derivative as

$$F'(\phi_{i,j}) \equiv \frac{dF}{d\phi_{i,j}} = \frac{F(\phi_{i,j}+\delta) - F(\phi_{i,j})}{\delta} \tag{4.12}$$

Once we have both $F(\phi_{i,j})$ and $F'(\phi_{i,j})$ it is possible to calculate a value for the potential $\bar{\phi}_{i,j}$ that will depend also upon the potentials at neighboring points,

$$\bar{\phi}_{i,j} = \phi_{i,j} - \frac{F(\phi_{i,j})}{F'(\phi_{i,j})} \tag{4.13}$$

The new value of the potential at (i, j) is then determined, according to the relaxation coefficient w, as

$$\phi_{i,j,\text{new}} = \phi_{i,j} + (\bar{\phi}_{i,j} - \phi_{i,j})\, w = \phi_{i,j} - w \frac{F(\phi_{i,j})}{F'(\phi_{i,j})} \tag{4.14}$$

After the new value for the potential is determined in this way, we can either save it in a temporary array until the calculation is finished for all the grid points or else update it immediately in the array of current potentials. The second method usually achieves faster convergence. During the relaxation this process is executed for all the inner points of the grid in each iteration. When it has converged we get the potential values that solve the equations. We then use this solution to calculate the effective conductivity and the other coefficients of the EMA.

The parameters that were held fixed during all the calculations are the conductivity of the host $\sigma_0 = 1$ and the ratio between the radius of the inclusion and that of the host $R_1/R_0 = 0.1$. The parameters that were allowed to change are the nonlinearity coefficient β, the conductivity of the inclusion σ_1, and the number of points in the grid.

4.3. Tests of the Algorithm

Two sets of numerical computations were made in order to test the algorithm. Both calculations were for cases where we could estimate the results using other methods and compare them to the numerical ones.

4.3.1. Calculation for Linear Conductivity. In the linear case $\beta = 0$ the bulk effective conductivity σ_e can be calculated in closed form if the radius of the spherical host is infinite. The potentials in the host and in the inclusion were expressed using Legendre functions as

$$\phi_0(r, \theta) = \left(Ar + B\frac{1}{r^2} \right) \cos\theta \qquad \text{in the host} \tag{4.15}$$

$$\phi_1(r, \theta) = Cr \cos\theta \qquad \text{in the inclusion} \tag{4.16}$$

In order to find the three unknowns A, B, and C we need three equations. Two of those are obtained from the continuity condition on the polar component of **E** and on the radial component of **D**. The third equation comes from the boundary condition at large distances $\phi_0(r, \theta) = -E_0 r \cos\theta$ for $r \to \infty$. From the solution we calculated $f(0)$, $f(\infty)$, a, and b by integrating Eqs. (2.8), (2.11), (2.9), and (2.12). The expressions obtained for a and b do not depend on R_0, but the expressions for $f(0)$ and $f(\infty)$ do. We assume that this solution is a good approximation even for a finite large host. Therefore we substitute a finite value of R_0 in the expressions and get an estimated analytical solution for the same configuration that we solve numerically.

The numerical calculations for the linear case were executed using two different contrasts, namely $\sigma_1 = 10^{12}$ and $\sigma_1 = 10^{-12}$. Different grid sizes were used from 101 to 701 points in each direction. As expected, the results indicate that the numerical coefficients are closer to the estimated analytical ones for the denser grids. Moreover, adding points in the r direction improves the results more effectively than adding points in the θ direction. Since the remaining calculations are all executed using grids of 101×101 points, we compare results for the present calculation using such a grid with the analytical results in Table I.

The fact that even in the analytical calculation the EMA percolation threshold is not exactly 1/3 is due to the fact that the ratio R_0/R_1 was 10 instead of ∞. On the other hand, the analytical values for a and b are accurate, since they are calculated using integration over the inclusion and therefore do not depend on the size of the host.

From the table we conclude that for the grid size used we get very good results for the extreme values of $f(x)$ and for p_c, but that the evaluation of

Table I. Numerical Computations Compared to Analytical Results for the Linear Case of an Isolated Spherical Inclusion

Calculated coefficient	Analytical value	Numerical value
$\sigma_e(\sigma_1 \to 0)$	0.9984995	0.998522...
$\sigma_e(\sigma_1 \to \infty)$	1.002998	1.003014...
$f(\infty)$	−1.5005	−1.48176...
$f(0)$	2.998	3.021215...
b	2.25	2.477179...
a	9	7.455764
p_c	0.333556...	0.329063...

a and b is less accurate. When we used the denser grids the values obtained for a, b were considerably more accurate.

4.3.2. The Low Contrast Case. When the distribution of component conductivities is very narrow, $\delta\sigma_i \equiv (\sigma_i - \langle\sigma\rangle) \ll \langle\sigma\rangle$, the bulk effective conductivity σ_e can be expanded through second order in $\delta\sigma_i$ even in the nonlinear case.[6] For a single spherical inclusion σ_1 of radius R_1 at the center of a larger sphere σ_0 of radius R_0 this expansion leads to $(x \equiv \sigma_0/\sigma_1)$

$$\sigma_e = 1 + \left(\frac{R_1}{R_0}\right)^3 \left(\frac{1}{x} - 1\right) - \frac{\beta+2}{2\beta}\left(1 - \frac{\arcsin\sqrt{\beta/(\beta+1)}}{\sqrt{\beta}}\right)\left[\left(\frac{R_1}{R_0}\right)^3 - \left(\frac{R_1}{R_0}\right)^6\right]\left(\frac{1}{x} - 1\right)^2 + \mathcal{O}\left[\left(\frac{1}{x-1}\right)^3\right] \tag{4.17}$$

As a further test of our numerical algorithm we compared numerical calculations for this case with the results of this expression. The calculations were made for values of $\beta = 1, 2, 3, 4$ and for values of $x = \sigma_0/\sigma_1 = 1.1$, 1.01, 1.001, 1.0001, 1.00001. Since the results for the different values of β were all alike, we present results only for one value of β. In Table II we show $1 - \sigma_e/\sigma_0$ for different values of $x = \sigma_0/\sigma_1$ when $\beta = 4$.

In this table the relative difference between the numerical result and the asymptotic approximation increases as x approaches 1. For $x \geqslant 1.001$ those differences are mostly attributable to the neglected terms in (4.17). When $|1 - x| < 10^{-3}$ those differences indicate the limits of accuracy of the numerical algorithm, which are due to the finite grid size.

Table II. Numerical Computations Compared to Analytical Results for $1-\sigma_r/\sigma_0$ in the Low-Contrast Case When $\beta=4$

$x=\sigma_0/\sigma_1$	Numerical value	Value from (4.17)
1.1	9.35×10^{-5}	9.37×10^{-5}
1.01	9.86×10^{-6}	9.93×10^{-6}
1.001	9.75×10^{-7}	9.99×10^{-7}
1.0001	6.30×10^{-8}	10.0×10^{-8}
1.00001	-3.90×10^{-8}	10.0×10^{-9}

4.4. Calculation of the Coefficients

The aim of the main set of calculations was to compute the coefficients for different values of the nonlinearity exponent β. In all the calculations the conductivity of the host was $\sigma_0=1$ and the conductivity of the inclusion varied from 10^{-12} to 10^{12} in factor-10 steps. The calculations were executed both for positive values of $\beta=1, 2, 3, 4$ and for negative ones $\beta=-0.2, -0.4, -0.6$. The number of iterations required changed with the values of β and σ_1. In general the number of iterations was bigger for smaller values of β and for bigger values of σ_1.

Figure 5 shows the calculated effective conductivity versus $x=\sigma_0/\sigma_1$ for different values of beta. The results indicate that the effective conductivity is closer to 1 for smaller values of β.

During the relaxation, at the end of each iteration, a total error was calculated as the integral of $|\nabla\cdot\mathbf{J}|$. Every time that the error decreased by a given amount a new value was calculated for each of the coefficients. If the pth computed value of a certain coefficient C is denoted by C_p, then the difference between the current value and the previous value is $\Delta C_p=C_p-C_{p-1}$ and the ratio between two consecutive differences is $m_p=\Delta C_p/\Delta C_{p-1}$. It was found that in most cases this ratio does not increase with p; therefore an extrapolated difference or increment $C_\infty-C_p$ could be calculated as follows:

$$\begin{aligned} C_\infty-C_p &= \Delta C_{p+1}+\Delta C_{p+2}+\cdots \\ &= \Delta C_p(m_{p+1}+m_{p+1}m_{p+2}+\cdots) \\ &\cong \Delta C_p\frac{m_p}{1-m_p}=\Delta C_p\left(\frac{1}{1-m_p}-1\right) \end{aligned} \tag{4.18}$$

These extrapolated increments were used to decide when to terminate the iterations. Moreover, after termination they were added to each coefficient

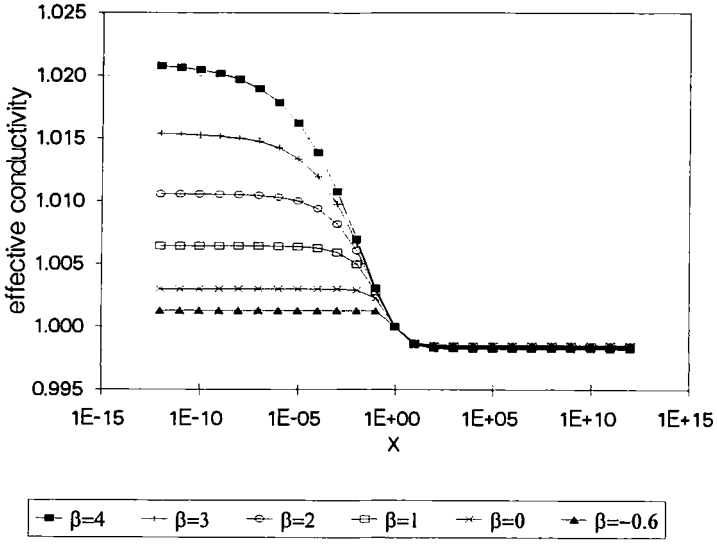

Fig. 5. Calculated effective conductivity σ_e plotted as a function of $x = \sigma_0/\sigma_1$ for different values of beta.

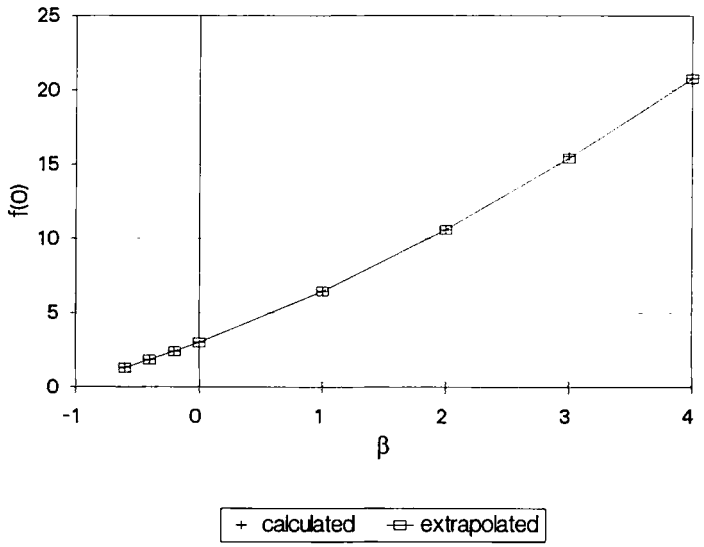

Fig. 6. Values of $f(0)$ plotted as a function of β. The values that were calculated directly from the final potential are the crosses, and the extrapolated values are the empty squares.

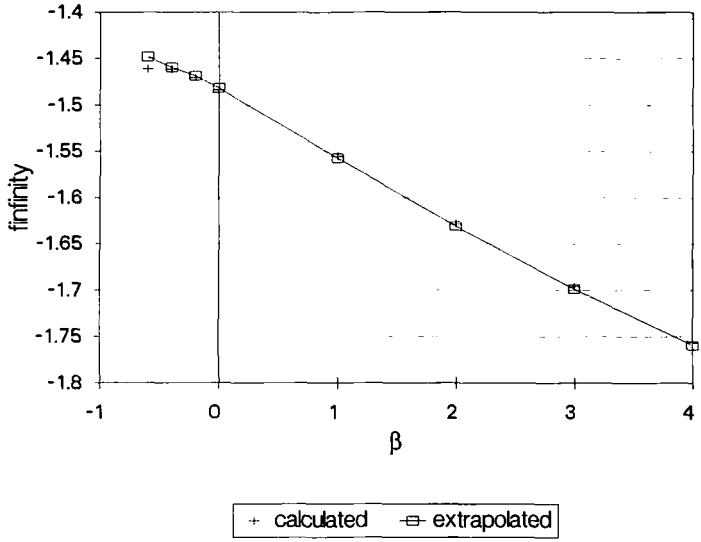

Fig. 7. Values of $f(\infty)$ plotted as a function of β. The values that were calculated directly from the final potential are the crosses, and the extrapolated values are the empty squares.

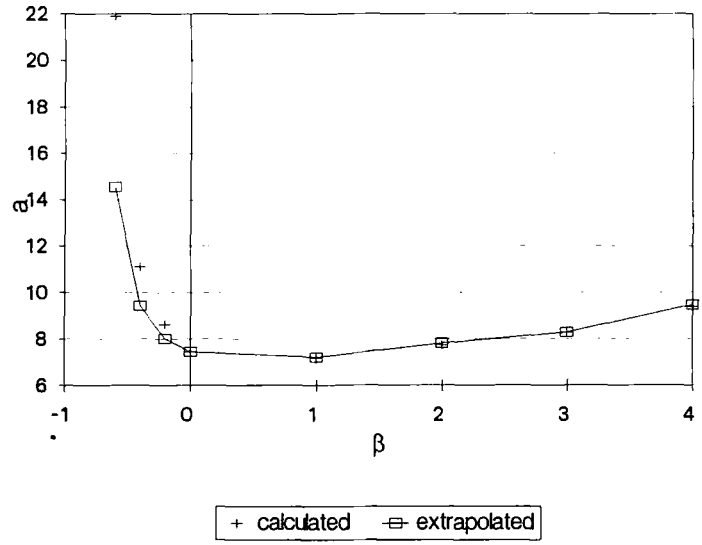

Fig. 8. Values of a plotted as a function of β. The values that were calculated directly from the final potential are the crosses, and the extrapolated values are the empty squares. Note the difference between the values for negative β.

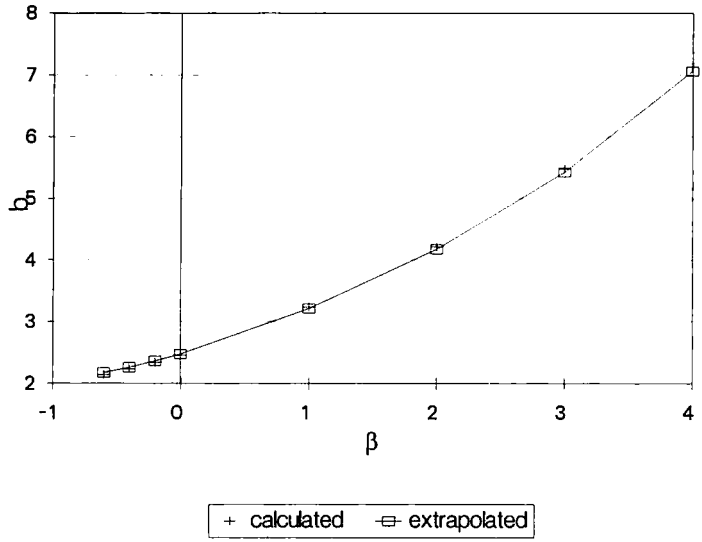

Fig. 9. Values of b plotted as a function of β. The values that were calculated directly from the final potential are the crosses, and the extrapolated values are the empty squares.

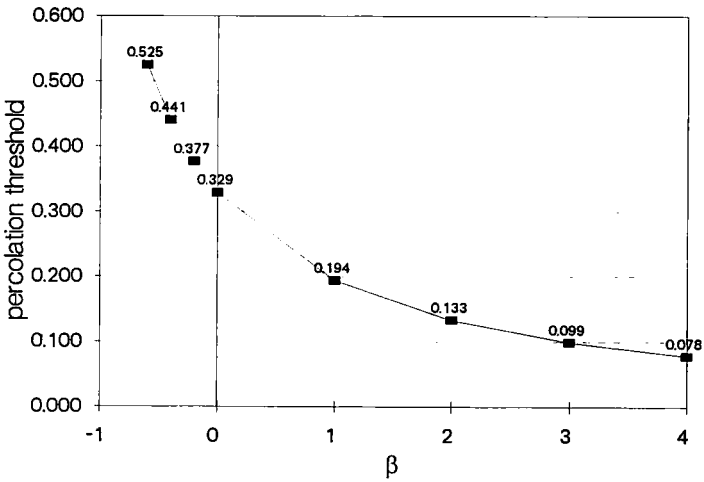

Fig. 10. The calculated percolation threshold plotted as function of β for a continuum system.

in order to obtain an extrapolated value. The following figures show the coefficients calculated in this way. Figures 6–9 show the values of $f(0)$, $f(\infty)$, a, and b as function of β. Two values are shown for each coefficient. One was calculated directly from the final potential distribution, while the second is the extrapolated value. Evidently there is a significant difference between the two values only in the case of a, and even then only for $\beta < 0$. Note that the agreement of the two results only indicates good convergence of the relaxation procedure and not whether the results are accurate: Inaccuracies due to the finite grid size in fact cause a, b to be rather inaccurate in the case $\beta = 0$, as was explained earlier in connection with Table I. Using (2.6), we calculated p_c for the different values of β. The results are plotted in Fig. 10.

The effective conductivity was calculated in all cases. Using its value, we calculated the function $f(x)$ according to (2.4) for all values of x that were used. The values of this function make it possible to calculate an EMA effective conductivity for a nonlinear composite medium using (2.5) even when the contrast between the conductivities is not extreme. The calculated values of $f(x)$ are displayed in Fig. 11. We tried to compare these values with the asymptotic expressions (2.7), (2.10) for small and large x. For small x the agreement was very good, but not for large x: Due to the smallness of the b/x term in (2.10), in practice its contribution is usually overshadowed by the errors in the numerical evaluations of $f(x)$ and $f(\infty)$, which are both of order $V_a/V \cong 10^{-3}$.

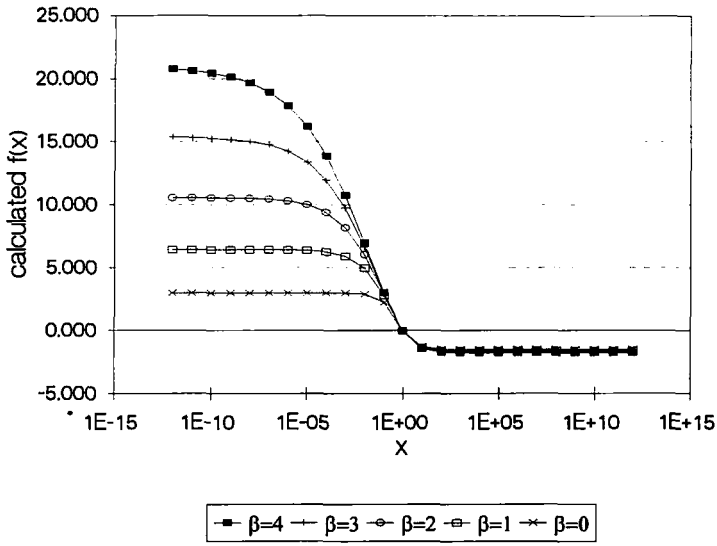

Fig. 11. Numerically calculated values for $f(x)$ as a function of x for different values of β in continuous media.

Table III. Numerical Calculations of the Coefficients Compared to Results of Variational Calculations for $\beta = 2$

Calculated coefficient	Our value	Ref. 15
$f(\infty)$	−1.6308...	−0.4814
$f(0)$	10.6104...	1
b	4.1810...	1.4567
a	7.8149...	1.333...

When we compare the results for a, b, $f(0)$, $f(\infty)$, and p_c obtained for the the continuum composite system to the results obtained for the discrete network model a striking fact emerges: Whereas in the linear case ($\beta = 0$) the results are identical, in the nonlinear cases they are not only different, but sometimes exhibit *opposite behavior* as function of β. Thus, in the continuum system a increases and p_c decreases with increasing β (see Figs. 1 and 2), while in the network model a decreases and p_c increases with increasing β (see Figs. 8 and 10).

A different approach has recently been used to calculate the coefficients for the nonlinear EMA.[15] In that approach, trial functions based on solution of a linear problem were used to approximate the potential for a nonlinear composite with $\beta = 2$. These had some free parameters that were determined by minimizing an energy integral like (2.2). The optimized trial functions were used to estimate the values of $f(x)$ for very large and very small x, and consequently to obtain values for $f(0)$, $f(\infty)$, a, and b. The values of the coefficients which we obtained in the numerical calculations for $\beta = 2$ are very different from the ones found in ref. 15 using the variational method, as shown in Table III.

We conclude that the use of linear solution trial functions apparently leads to unacceptably large errors in the calculation of these coefficients.

5. DISCUSSION

In this work, a nonlinear partial differential equation was solved numerically in order to calculate certain coefficients and the function $f(x)$ for the effective medium approximation of nonlinear composite media. The coefficients obtained for the linear case $\beta = 0$ mostly compared very well with analytically calculated coefficients. Also, the results for a low-contrast nonlinear case were compared to analytical results with excellent agreement. It was shown that, if more precise results are required, then the discretizing grid in (r, θ) must be made more dense, particularly in the r direction.

We also developed a similar EMA for nonlinear conductance networks and calculated (numerically) the various coefficients and the function $f(x)$. In contrast with the situation in linear systems ($\beta = 0$), a comparison of the continuum and the network result shows that they are quite different, sometimes even in their qualitative behavior as functions of β. These differences deserve further study. They indicate that the use of discrete network models for nonlinear continuum composites should be pursued with great caution.

ACKNOWLEDGMENT

The research reported here was supported in part by a grant from the US–Israel Binational Science Foundation.

REFERENCES

1. D. Stroud and P. M. Hui, *Phys. Rev. B* **37**:8719 (1988).
2. X. C. Zeng, D. J. Bergman, P. M. Hui, and D. Stroud, *Phys. Rev. B* **38**:10970 (1988).
3. X. C. Zeng, P. M. Hui, D. J. Bergman, and D. Stroud, *Physica A* **157**:192 (1989).
4. R. R. Tremblay, G. Albinet, and A.-M. S. Tremblay, *Phys. Rev. B* **45**:755 (1992).
5. O. Levy and D. J. Bergman, *Phys. Rev. B* **50**:3652 (1994).
6. R. Blumenfeld and D. J. Bergman, *Phys. Rev. B* **40**:1987 (1989).
7. P. Ponte Castañeda, G. deBotton, and G. Li, *Phys. Rev B* **46**:4387 (1992).
8. K. W. Yu and G. Q. Gu, *Phys. Lett. A* **193**:311 (1994).
9. K. W. Yu and G. Q. Gu, *Phys. Lett. A* **205**:295 (1995).
10. D. A. G. Bruggeman, *Ann. Phys.* (Leipzig) **24**:636 (1935).
11. D. J. Bergman, In *Composite Media and Homogenization Theory*, G. Dal Maso and G. F Dell'Antonio, eds. (Birkhäuser, Boston, 1991), pp. 67–79.
12. A. Aharony and D. Stauffer, *Introduction to Percolation Theory*, 2nd ed. (Taylor and Francis, London, 1992).
13. W. H. Press, S. A. Teukolsky, W. T. Vetterling, and B. P. Flannery, *Numerical Recipes in C*, 2nd ed. (Cambridge University Press, Cambridge, 1992), pp. 863–866.
14. S. Kirkpatrick, *Rev. Mod. Phys.* **45**:573 (1973).
15. H. C. Lee and K. W. Yu, *Phys. Lett. A* **197**:341 (1995).